ISSN 2072-5981

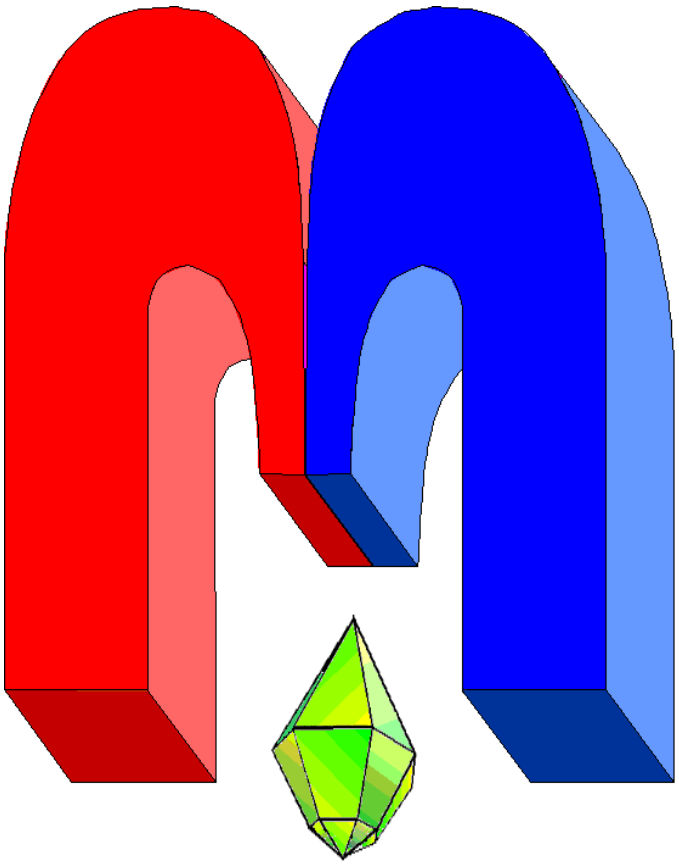

Magnetic Resonance in Solids

Electronic Journal

Volume ***18,***
Issue ***2***
Paper No ***16207,***
1-8 pages
2016

http://mrsej.kpfu.ru
http://mrsej.ksu.ru

Established and published by Kazan University
Sponsored by International Society of Magnetic Resonance (ISMAR)
Registered by Russian Federation Committee on Press, August 2, 1996
First Issue was appeared at July 25, 1997

"***Magnetic Resonance in Solids. Electronic Journal***" (**MRS*ej***) is a peer-reviewed, all electronic journal, publishing articles which meet the highest standards of scientific quality in the field of basic research of a magnetic resonance in solids and related phenomena. **MRS*ej*** is free for the authors (no page charges) as well as for the readers (no subscription fee). The language of **MRS*ej*** is English. All exchanges of information will take place via Internet. Articles are submitted in electronic form and the refereeing process uses electronic mail. All accepted articles are immediately published by being made publicly available by Internet (http://**MRS*ej***.kpfu.ru).

* In Kazan University the Electron Paramagnetic Resonance (EPR) was discovered by Zavoisky E.K. in 1944.

Lithium diffusion in a new cathode material $Li_{0.8}[Ni_{0.6}Sb_{0.4}]O_2$ studied by ^{7}Li NMR†

T. Salikhov [1,*], E. Klysheva [1], E. Zvereva [2], V. Nalbandyan [3], I. Shukaev [3], B. Medvedev [3], E. Vavilova [1]

[1] Zavoisky Physical-Technical Institute of RAS, Sibirskii trakt 10/7, Kazan 420029, Russia

[2] Faculty of Physics, Moscow State University, Leninskie Gory 1-2, Moscow 119991, Russia

[3] Chemistry Faculty, Southern Federal University, Sorge 7, Rostov-on-Don 344090, Russia

**E-mail: tmsalikhov@gmail.com*

(Received December 10, 2016; accepted December 18, 2016)

A rhombohedral layered α-$NaFeO_2$-type compound, $Li_x[Ni_{(1+x)/3}Sb_{(2-x)/3}]O_2$ ($x = 0.8$) has been prepared from the sodium analogue by ion exchange at 570 K. In contrast to the stoichiometric composition $Li_3Ni_2SbO_6$, it shows considerable Li/Ni inversion and no long-range Ni/Sb ordering. The temperature dependence of the ^{7}Li NMR spin-lattice relaxation rate and linewidth data measured at temperature range from 30-450 K show the sharp increase of lithium ions mobility comparing to the stoichiometric compound $Li_3Ni_2SbO_6$. From the NMR data the activation energy was estimated by different methods.

PACS: 76.60.-k, 76.60.Es, 66.30.H-, 82.47.Aa, 82.56.Lz, 82.56.Na

Keywords: NMR, lithium, diffusion, cathode material

1. Introduction

Lithium-ion batteries play important role in energy storage and transport. They are widespread in modern life, from portable devices to electric vehicles. However, the rapid development of science and technology requires the creation of more and more effective energy storage devices. In particular, the positive electrode is responsible for such characteristics as energy density, safety, cost and toxicity. Therefore, the creation of new cathode materials is a key step for improving the effectiveness of the lithium batteries [1-3]. Most of today's cathode materials belong to the layered transition metal oxides, $LiCoO_2$ being the most widely used. However, materials based on Ni^{2+} are also of great interest because it is less expensive and less toxic than cobalt and provides possibility of a two-electron redox process. In particular, layered lithium nickel antimonates first prepared and characterized by our group in 2007 [4] attracted attention as possible positive electrode materials for Li-ion batteries [5-8].

Thereby, considering the charge/discharge characteristics of the battery, the ion diffusion and activation energies that describe Li-ion transport within cathode materials are of big interest. Nuclear magnetic resonance (NMR) is widely used for study the diffusion processes in ionic conductors, electrolytes and electrode materials [9-16]. The advantage of this method is the ability to study intragranular ion mobility without contribution from grain-boundary impedance that is very important for the investigation of polycrystalline materials. Furthermore, being a local method, NMR allows monitoring the characteristics of the ions on different structural positions selectively. However, the conventional NMR study of the ion diffusion is extremely difficult in magnetic materials since the interaction with magnetic ions in the lattice strongly affects Li-NMR parameters even in a paramagnetic state [17, 18].

In this work, we have studied the diffusion of lithium ions in the cathode material with Li vacancies. For this purpose, we synthesized two compositions $Li_x[Ni_{(1+x)/3}Sb_{(2-x)/3}]O_2$: one Li-deficient ($x = 0.8$) and, for comparison, another one with completely filled Li sites ($x = 1$). The investigation of the lithium mobility was done by NMR technique modified for better quality of measurements in the paramagnetic compounds.

† This paper material was selected at XIX International Youth Scientific School "Actual problems of magnetic resonance and its application", Kazan, 24 – 28 October 2016. The paper was recommended to publication in our journal and it is published after additional MRSej reviewing.

2. Experimental

2.1 Sample preparation and characterization

In contrast to the sodium analogue [19] and stoichiometric $Li_3Ni_2SbO_6$ [20], its cation-deficient solid solutions, $Li_x[Ni_{(1+x)/3}Sb_{(2-x)/3}]O_2$, $x < 1$, could not be prepared by direct high-temperature synthesis. Therefore, $Na_{0.8}Ni_{0.6}Sb_{0.4}O_2$ was prepared first as described previously [19]. Reagent-grade antimonic acid, hydrous nickel oxide (both analyzed gravimetrically) and dried sodium carbonate were mixed thoroughly, pressed, reacted at 1070 K and, after regrinding and pressing, sintered at 1380 K for 3 h within the sacrificial packing powder of the same composition. 3 % sodium excess was employed to compensate for volatilisation at the high temperature.

Phase-pure sodium samples were ion-exchanged in 20-fold excess molten $LiNO_3$ to give $Li_{0.8}Ni_{0.6}Sb_{0.4}O_2$. The sintered discs and those ground to powder were treated at 610 K for 4 h and at 570 K for 3 h, respectively, and then washed and dried. The discs were porous and this enabled complete exchange in the bulk, as confirmed by the X-ray diffraction (XRD) powder analysis of a crushed sample. For comparison, a pellet of stoichiometric $Li_3Ni_2SbO_6$ [20] was sintered at 1370 K. All samples were light green, excluding any possibility of a mixed-valence state of nickel that always gives rise to dark coloration even at low fractions of Ni^{3+} (<< 1%).

The XRD phase analysis was performed in CuKα radiation using an ARL X'TRA diffractometer equipped with a solid-state Si(Li) detector. The higher-intensity data for the structural analysis of $Li_{0.8}Ni_{0.6}Sb_{0.4}O_2$ were collected using a rotating-anode Rigaku instrument with a secondary-beam graphite monochromator, also in copper radiation. Structural analysis was performed by the Rietveld method implemented in GSAS+EXPGUI suite [21, 22].

2.2 Magnetic susceptibility measurements

Magnetic susceptibility measurements were done by means of a Quantum Design Magnetic Property Measurement System (MPMS) XL-7 magnetometer. The temperature dependencies of the magnetic susceptibility were measured at a magnetic field $B = 0.7$ T in the temperature range 2-350 K.

2.3 NMR measurements

Nuclear magnetic resonance (NMR) experiments were carried out using Tecmag solid-state pulse spectrometer and Bruker resistive 0-1.5 T magnet at the frequency 12 MHz. The NMR signals were observed on ^7Li nuclei with spin $I = 3/2$ and gyromagnetic ratio $\gamma N/2\pi = 16.546$ MHz/T. The NMR spectra were obtained either by Fourier transformation of the NMR solid-echo signal at a fixed field of $H = 0.724$ T or by step-by-step sweeping the field and integrating the solid-echo signal at each field step. ^7Li spin-lattice relaxation rate $1/T_1$ was measured using a stimulated echo pulse sequence. ^7Li relaxation rate $1/T_2$ was obtained by measuring the solid-echo integral as a function of τ, where τ is time between two $\pi/2$ pulses. In the temperature range from 30 K to 450 K a home-made low temperature and high temperature thermostats and probes was used.

3. Results

3.1 Crystal structure

Similar to the sodium precursor, XRD pattern of $Li_{0.8}Ni_{0.6}Sb_{0.4}O_2$ was completely indexed on the basis of a small rhombohedral unit cell of the α-$NaFeO_2$ type. No superlattice reflections indicating long-range Ni/Sb ordering characteristic of the $x = 1$ sample ($Li_3Ni_2SbO_6$) could be found. Instead, an elevated background is observed in the same angular range ($2\Theta = 19$-$24°$, Fig. 1) indicating that short-range order does exist. The XRD pattern may be found in the PDF database [4].

The crystal structure was successfully refined within the space group $R\bar{3}m$ and refinement results are shown in Fig. 1. The most interesting result of the refinement is considerable degree of Li/Ni inversion: about 8 % Li was found on Ni site and *vice versa*, similar to $Li_3Cu_2SbO_6$, also prepared by the low-temperature ion exchange, where 16 % Li was found on Cu site [23].

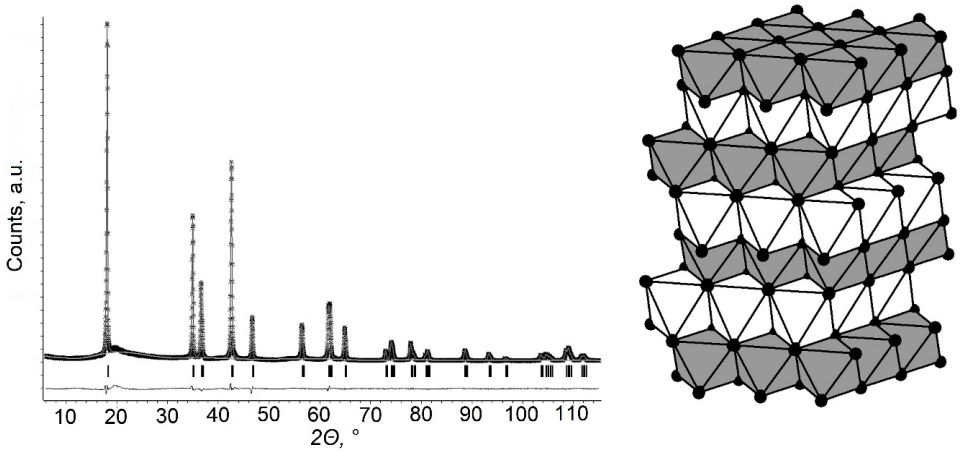

Figure 1. Results of the Rietveld refinement of $Li_{0.8}Ni_{0.6}Sb_{0.4}O_2$. XRD profile (left): asterisks, experimental points; line, calculated profile; line at the bottom, difference plot; vertical bars, Bragg positions. Polyhedral view of the crystal structure (right): gray octahedra, $(Ni,Sb)O_6$ with small admixture of Li; white octahedra, LiO_6, partially occupied, with small admixture of Ni.

3.2 Magnetic susceptibility

The temperature dependence of the magnetic susceptibility $\chi = M/B$ for $Li_{0.8}Ni_{0.6}Sb_{0.4}O_2$ measured at $B = 0.7$ T is shown in Fig. 2. Overall the $\chi(T)$ dependence manifests a Curie-Weiss-type behavior upon a decrease of temperature. At low temperatures the $\chi(T)$ deviates from the Curie-Weiss law but still does not show any sign of long-range magnetic ordering down to 2 K. Obviously, these data are cardinally different from those detected for stoichiometric compound $Li_3Ni_2SbO_6$ [20, 24] indicating the new type of magnetic properties which should be expected for this new compound. The high-temperature part of $\chi(T)$ was fitted in accordance the Curie-Weiss law with addition of a temperature-independent term χ_0:

$$\chi = \chi_0 + \frac{C}{T - \theta}, \qquad (1)$$

where θ is the Weiss temperature, C is the Curie constant $C = N_A \cdot \mu_{eff}^2 \cdot \mu_B^2 / 3k_B$, N_A is Avogadro's number, μ_{eff} is the effective magnetic moment, μ_B is Bohr's magneton, and k_B is Boltzmann's constant. The best fit of experimental data yields the following parameters: $\theta \approx -4$ K, $C \approx 0.97$ emu/mol K and $\chi_0 \approx 2.8 \cdot 10^{-4}$ emu/mol. The effective magnetic moment calculated from the Curie constant is about $\mu_{eff} \approx 2.7\ \mu_B$ /f.u. Relatively large positive value of temperature-independent term indicates non-negligible Van-Fleck contribution from Ni^{2+} similarly to native compound $Li_3Ni_2SbO_6$ [20, 24]. At the same time the Weiss temperature θ takes here a negative value, which indicates the predomination of the antiferromagnetic interactions in $Li_{0.8}Ni_{0.6}Sb_{0.4}O_2$ and again points to the clear difference between our sample and the stoichiometric compound $Li_3Ni_2SbO_6$ [24].

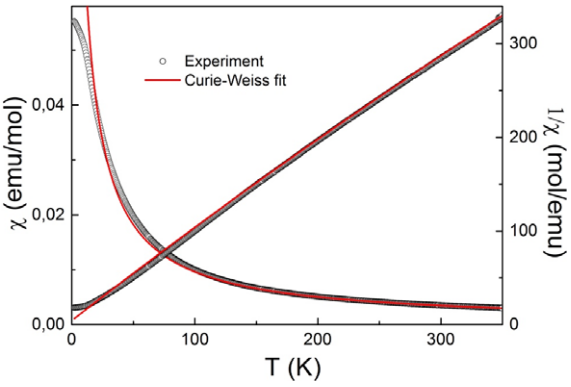

Figure 2. The dependence of the magnetic susceptibility of $Li_{0.8}Ni_{0.6}Sb_{0.4}O_2$ at $B = 0.7$ T as a function of temperature.

3.3 NMR Spectra

For the quadrupolar ^{7}Li ($I = 3/2$) nucleus, one can expect two satellite lines and the central line in the single crystal corresponding to three allowed transitions, the powder spectra usually demonstrate the averaged profile of the satellites. As shown in Fig. 3, in the $Li_{0.8}Ni_{0.6}Sb_{0.4}O_2$ we observe only a single

spectral line without any satellites, which is conventional line shape for the case of small quadrupole splitting and the inhomogeneous line broadening. At the room temperature and up to 450 K the spectra have a Lorentzian shape and their positions are very close to the Larmor frequency. Upon lowering the temperature, the spectrum is shifted to the lower field and its shape changes to Gaussian. The line shift above 250 K is in order of magnitude of the external magnetic field inhomogeneity (10^{-4}) so the reliable parameter in this case is only the linewidth but not the line position. Fig. 4 shows the width of ^{7}Li NMR spectrum as a function of temperature. Below 250 K, the temperature dependence of the linewidth follows the temperature dependence of the static susceptibility indicating that the main origin of spectral broadening in this temperature region is a hyperfine coupling of the ^{7}Li nuclei with paramagnetic Ni^{2+} ions. Above 250 K, the additional line narrowing is observed. Investigation of the stoichiometric sample $Li_3Ni_2SbO_6$ demonstrates similar lineshape and linewidth behavior below 250 K, but no extra narrowing of the line up to the 450 K.

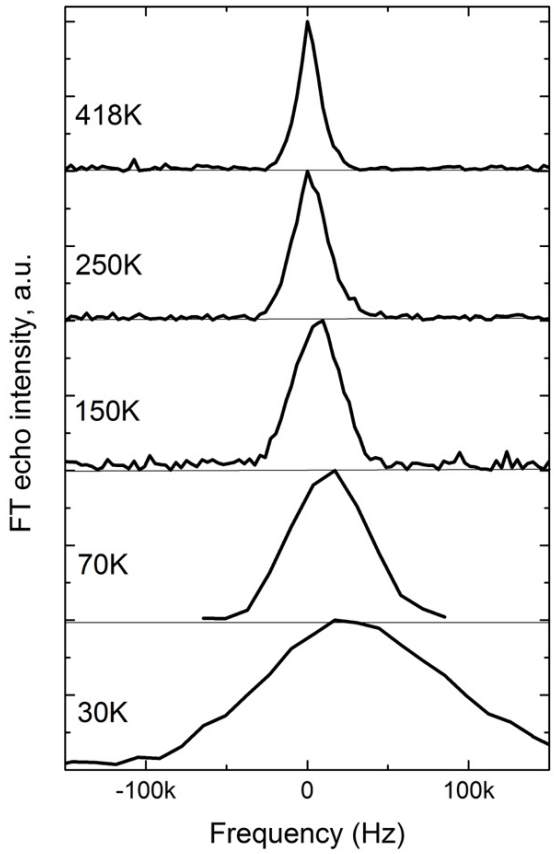

Figure 3. Temperature evolution of the ^{7}Li NMR spectra at 12 MHz.

3.4 NMR Relaxation

The decay of longitudinal magnetization was fitted well by a single exponential function (Fig. 5):

$$M_z = M_0\left(\exp\left\{-\frac{t}{T_1}\right\}\right). \qquad (2)$$

The good agreement with the experimental data proves that during the experiment all the transitions have exited but not only a main transition $(+1/2)-(-1/2)$ (in the last case, the relaxation process for spin 3/2 is described by two-exponential function)

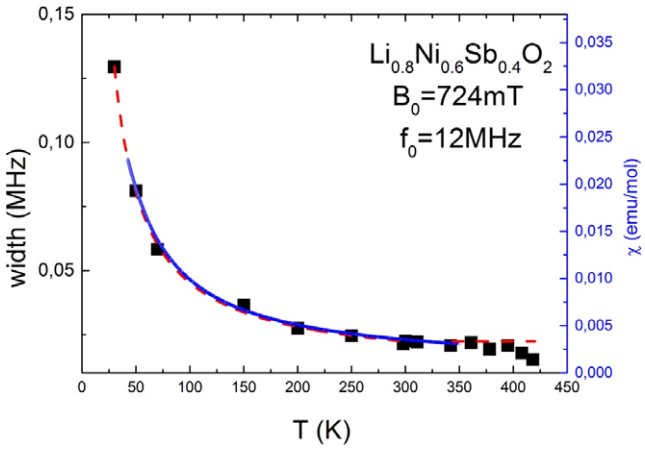

Figure 4. Temperature dependence of ^{7}Li NMR linewidth (square), the static susceptibility data (blue line) and fit according Curie-Weiss law (red line).

Here we can consider following mechanisms of relaxation: dipolar interaction of ^{7}Li nuclei and magnetic ions, dipolar interaction between nuclei, relaxation due to motion of ions and quadrupolar relaxation. Efficiency of relaxation mechanism depends of value of magnetic field at the position of nucleus and the proximity of the frequency of fluctuating field to Larmor frequency. The magnetic moment of Ni^{2+} ion is about 1000 times bigger than the magnetic moment of Li nucleus therefore the magnetic field induced by Ni ions is much bigger than one from lithium nuclei. At the same time the electron fluctuations slowdown in the neighborhood of the phase transition and their frequency becomes close to the Larmor frequency only at the very low temperatures. Relaxation due to the ion

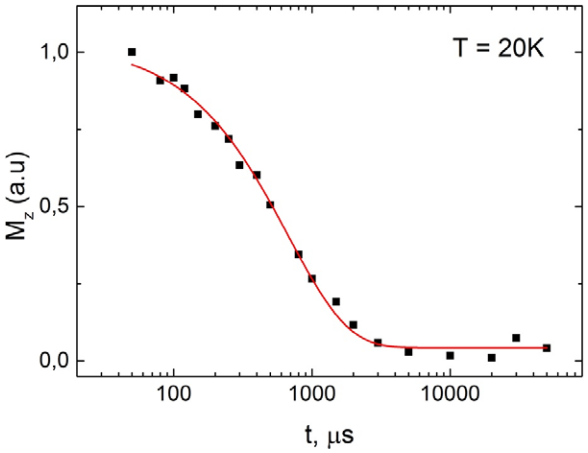

Figure 5. Time dependence of the ^{7}Li stimulated spin echo decay at $T = 20$ K. The solid line is a fit to Eq. (2).

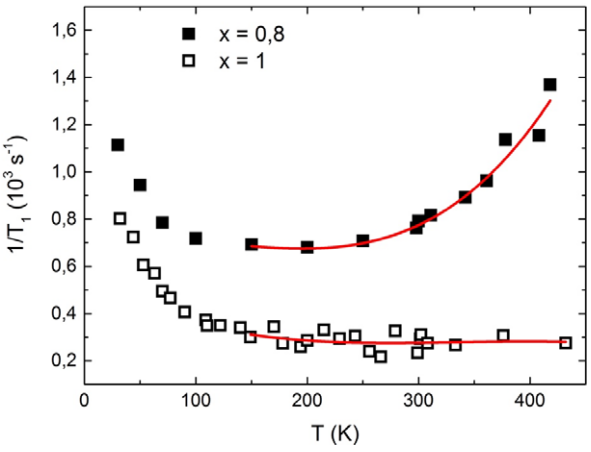

Figure 6. Temperature dependence of the ^{7}Li spin-lattice relaxation rate $1/T_1$, for $Li_3Ni_2SbO_6$ (open squares) and $Li_{0.8}Ni_{0.6}Sb_{0.4}O_2$ (solid squares) at frequency 12 MHz. Solid lines are guides for eye.

motion usually appears above the room temperature where the ions starts moving fast enough. Quadrupolar relaxation in our case is ineffective because a quadrupole splitting is very small, as shown in NMR spectra. Therefore, in further discussion we will consider only two contributions to the relaxation, which are resulting by interaction with magnetic ions and by lithium ion mobility.

The temperature dependence of the relaxation rate $1/T_1$ is shown in Fig. 6. At the temperatures 70 K < T < 250 K, $1/T_1$ is almost temperature-independent. At T > 250 K, the relaxation shows a slight growth at least up to 450 K. For the pristine compound $Li_3Ni_2SbO_6$ there is no significant change of the relaxation rate above 100 K up to 450 K (see Fig. 6).

4. Discussion

At the temperatures T > 300 K, the relaxation rate T_1^{-1} in $Li_{0.8}Ni_{0.6}Sb_{0.4}O_2$, increases (see Fig. 6) unlike the temperature-independent relaxation behavior in $Li_3Ni_2SbO_6$. The only reason for such dependence is a diffusion of Li ions appearing due to the vacancies in lithium positions in the non-stoichiometric sample that is favorable for lithium ion mobility. Spin-lattice relaxation in this case can be described by Bloembergen-Purcell-Pound theory (BBP) and reaches its maximum at the temperature where the correlation time τ_0 is equal to the $1/\omega_L$, where ω_L is a Larmor frequency. The correlation rate determined as a ion hopping rate obeys the Arrenius low:

$$\tau^{-1} = \tau_0^{-1}\left(\exp\left\{-\frac{E_a}{k_B T}\right\}\right), \tag{3}$$

where E_a is an activation energy. The relaxation rate due to the ion mobility for $T < T_{max}$ can be described [13] by formula:

$$\frac{1}{T_{1,diff}} = \omega_L^2\left(\exp\left\{-\frac{E_a}{k_B T}\right\}\right). \tag{4}$$

The total relaxation rate is the sum of the diffusion and magnetic contributions

$$T_1^{-1} = T_{1,diff}^{-1} + T_{1,mag}^{-1}. \tag{5}$$

The relaxation rate due to the interaction with magnetic ions moments is proportional to the temperature and the Ni^{2+} ion susceptibility [25-27], which obeys the Curie-Weiss law. When the temperature is much higher than Weiss parameter, we can assume $T_{1,mag}^{-1} = \text{const}$

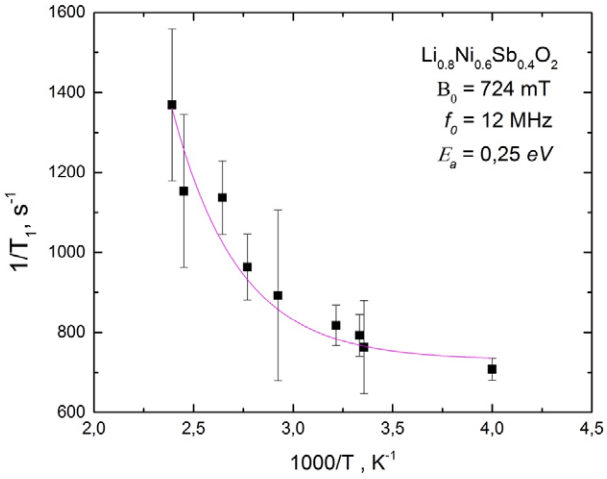

Figure 7. ^{7}Li spin-lattice relaxation rate as a function of 1000/*T*. The solid line shows the result of fitting according the Eq. (6).

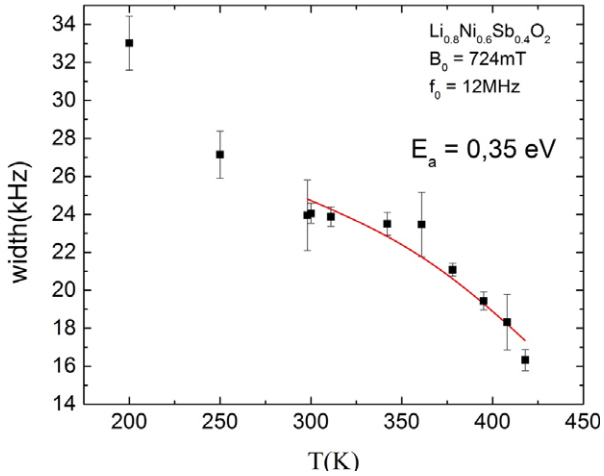

Figure 8. NMR linewidth as a function of temperature. The solid line is a fit by Eq. (7).

$$\frac{1}{T_1} = \omega_L^2 \left(\exp\left\{ -\frac{E_a}{k_B T} \right\} \right) + \text{const}, \tag{6}$$

where the constant value can be estimated as T_1^{-1} at $T \approx 200$ K. Similar procedure was proposed by Sugiyama et al. when interpreting the MuSR data of lithium diffusion in paramagnetic Li_2MnO_3 [28]. The value of the activation energy that can be obtained from the fitting of our experimental data is equal to 0.25 eV (Fig. 7). The maximum of the relaxation rate where $\tau_0 = 1/\omega_L$ is out of the temperature range of the measurement, so we cannot get the correlation rate value and the diffusion coefficient.

Another way to find activation energy is to investigate the temperature dependence of the NMR linewidth. At $T < 250$ K, the NMR line is inhomogeneously broadened due to the presence of the magnetic Ni ions creating a distribution of the quasi-static local fields in the sample. At high temperatures, with a developing of lithium ions mobility, the ion jump rate becomes bigger than the rigid lattice linewidth. At the fast mobility limit the hopping becomes so fast that lithium nuclei sense a uniform average local field. All nuclei have the same resonance frequency and so-called motional narrowing of the NMR line is observed. The temperature dependence of the linewidth can be used to get the activation energy value (see, for example, [29]). We used the formula proposed by Wilkening, Martin, et al. [15] for diamagnetics and modified it by adding the term $k\left(\frac{1}{T}\right)$ to the rigid line width, which takes into account broadening due to the interaction with paramagnetic ions and is proportional to Curie-Weiss susceptibility at high temperature limit:

$$\Delta\nu = \left(k\left(\frac{1}{T}\right) + \nu\Delta_R \right) \left[1 + \left(\frac{k\left(\frac{1}{T}\right) + \nu\Delta_R}{B} - 1 \right) \exp\left\{ -\frac{E_a}{k_B T} \right\} \right]^{-1} + C, \tag{7}$$

where $\Delta\nu$ is the line width of the central transition at temperature *T*, assuming as 1/3 of the total linewidth, $\nu\Delta_R$ and *B* are parameters, attributed to the line widths of the rigid lattice. *C* is additional linewidth caused by the inhomogeneity of the external static magnetic field which is almost temperature-independent above 300 K. Fit of the linewidth dependence on temperature shown at Fig. 8 gives an activation energy value about 0.35 eV.

A third way to obtain E_a is the empirical Waugh–Fedin expression [29]:

$$E_a = 1.617 \times 10^{-3} \times T_c, \tag{8}$$

here E_a is an activation energy in eV, T_c is onset of motional narrowing in K. Taking $T_c = 200$ K, we can determine $E_a = 0.323$ eV that is comparable to the activation energy value obtained from the linewidth temperature dependence but bigger than one from the relaxation rate slope. Authors of the works [15, 30, 31] notice that the phenomenological equation (7) and the empirical Waugh–Fedin expression (8) usually give the higher value of activation energy than the analysis of the relaxation rates dependence. This indicates that the lineshape investigations can give a correct order of magnitude of the activation energy but appropriate only for a rough estimation of the diffusion parameters in paramagnetic solids with ion mobility.

In view of these results, we may conclude that the vacancies on the lithium positions, which are formed in the samples of $Li_{0.8}Ni_{0.6}Sb_{0.4}O_2$, are actually favorable for ion mobility in the system. The activation energy value obtained from temperature dependence of spin-lattice relaxation rate and NMR linewidth is comparable with the results gotten by other methods for layered lithium contained compounds [5, 32]. On the other hand, we cannot get the correlation rate value and the diffusion coefficient and obtain the information about possible diffusion pathways from our experiments due to the limited range of the achieved temperatures. The measurements of the relaxation in the rotated frame can give an opportunity to solve this problem.

Acknowledgements

This work was supported by grants 14-03-01122 (I.S. and V.N.), 14-02-00245 (E.Z.) and 14-02-01194 (T.S. and E.V.) from Russian Foundation for Basic Research. Initial XRD characterization of $Li_{0.8}Ni_{0.6}Sb_{0.4}O_2$ was supported by the Grant-in-Aid 00-15 from the International Centre for Diffraction Data. The authors also thank Dr. S.N. Polyakov for the Rigaku scan.

References

1. Croguennec L., Palacin M.R. *J. Am. Chem. Soc.* **137**, 3140-3156 (2015)
2. Crabtree G., Kocs E., Trahey L. *MRS Bull*. **40**, 1067-1076 (2015)
3. Bensalah N., Dawood H. *J. Mater Sci. Eng.* **5**, 1000258 (2016)
4. Powder Diffraction File, Philadelphia, ICDD, 2007, cards 00-57-219 ($Li_3Ni_2SbO_6$) and 00-57-861 ($Li_{0.8}Ni_{0.6}Sb_{0.4}O_2$).
5. Ma X., Kang K., Ceder G., Meng Y.S. *J. Power Sources* **173**, 550–555 (2007)
6. Cui P., Jia Z., Li L., He T. *J. Phys. Chem. Solids* **72**, 899-903 (2011)
7. Twu N., Li X., Urban A., Balasubramanian M., Lee J., Liu L., Ceder G. *Nano Lett*. **15**, 596-602 (2015)
8. Yang Z., Zhang Z., Pan Y., Zhao S., Huang Y., Wang X., Chen X., Wie S. *J. Solid State Chem.* **244**, 52-60 (2016)
9. Langer J., Wilkening M. *Solid State Ionics* **293**, 85-93 (2016).
10. Nakhal S., Wiedemann D., Stanje B., Dolotko O., Wilkening M., & Lerch M. *J. Solid State Chem.* **238**, 60-67 (2016)
11. Walter S., Wilkening M. *Solid State Ionics* **287**, 77-82 (2016)
12. Wohlmuth D., Epp V., Wilkening M. *ChemPhysChem* **16(12)**, 2582-2593 (2015)
13. Heitjans P., Kärger J., eds. *Diffusion in condensed matter: methods, materials, models.* Springer Science & Business Media (2006)
14. Paris M.A., Sanz J., Leon C., Santamaría J., Ibarra J., Várez A. *Chemistry of materials* **12(6)**, 1694-1701 (2000)
15. Wilkening M., Bork D., Indris S., Heitjans P. *Phys. Chem. Chem. Phys.* **4(14)**, 3246-3251 (2002)

16. Verhoeven V.W.J., De Schepper I.M., Nachtegaal G., Kentgens A.P.M., Kelder E. M., Schoonman J., Mulder F.M. *Phys. Rev. Lett.* **86(19)**, 4314 (2001)
17. Grey C.P., Dupré N. *Chem. Rev.* **104(10)**, 4493-4512 (2004)
18. Tomeno I., Oguchi M., *J. Phys. Soc. Jpn*. **67**, 318 (1998)
19. Politaev V.V., Nalbandyan V.B., Petrenko A.A., Shukaev I.L., Volotchaev V.A., Medvedev B.S. *J. Solid State Chem.* **183**, 684-691 (2010)
20. Zvereva E.A., Evstigneeva M.A., Nalbandyan V.B., Savelieva O.A., Ibragimov S.A., Volkova O.S., Medvedeva L.I., Vasiliev A.N., Klingeler R., Büchner B. *Dalton Trans.* **41(2)**, 572-580 (2012)
21. Larson A.C., Von Dreele R.B., General Structure Analysis System (GSAS), Los Alamos National Laboratory Report LAUR86-748 (2004).
22. Toby B.H. *J. Appl. Cryst.* **34**, 210-213 (2001)
23. Koo C., Zvereva E.A., Shukaev I.L., Richter M., Stratan M.I., Vasiliev A.N., Nalbandyan V.B., Klingeler R. *J. Phys. Soc. Japan* **85**, 084702 (2016)
24. Zvereva E.A., Stratan M.I., Ovchenkov Y.A., Nalbandyan V.B., Lin J.Y., Vavilova E.L., Iakovleva M.F., Abdel-Hafiez M., Silhanek A.V., Chen X.-J., Stroppa A., Picozzi S, Jeschke H.O., Valentí R. Vasiliev A.N. *Phys. Rev. B.* **92**, 144401 (2015)
25. Iakovleva M.F., Vavilova E.L., Grafe H.J., Maljuk A., Wurmehl S., Büchner B., Kataev V. *Appl. Magn. Reson.* **47**, 727 (2016)
26. Arango Y.C., Vavilova E., Abdel-Hafiez M., Janson O., Tsirlin A.A., Rosner H., Drechsler S.-L., Weil M., Nénert G., Klingeler R., Volkova O., Vasiliev A., Kataev V., Büchner B. *Phys. Rev. B* **84(13)**, 134430 (2011)
27. Moriya T. *Progress of Theoretical Physics* **16(1**), 23-44 (1956)
28. Sugiyama J., Mukai K., Nozaki H., Harada M., Månsson M., Kamazawa K., Andreica D., Amato A., Hillier A.D. *Phys. Rev. B* **87(2)**, 024409 (2013)
29. Heitjans P., Indris S. *J. Physics: Condens. Matter* **15(30)**, R1257 (2003)
30. Waugh J.S., Fedin E.I. *Soviet Physics-Solid State* **4(8)**, 1633-1636 (1963)
31. Kuhn A., Narayanan S., Spencer L., Goward G., Thangadurai V., Wilkening M. *Phys. Rev. B* **83(9)**, 094302 (2011)
32. Okubo M., Tanaka Y., Zhou H., Kudo T., Honma I. *J. Phys. Chem, B* **113(9)**, 2840-2847 (2009)